

Tunable magnetic interactions in LaAlO₃/SrTiO₃ heterostructures by ionic liquid gating

Chunhai Yin, Kumar Prateek, Wouter Gelling and Jan Aarts
*Huygens-Kamerlingh Onnes Laboratory,
Leiden University, P.O. Box 9504,
2300 RA Leiden, The Netherlands*

(Dated: April 26, 2019)

The gating effect achieved by an ionic liquid and its electric double layer allows for charge transfer which can be an order of magnitude larger than with conventional dielectrics. However, the large charged ions also causes inevitable Coulomb scattering in the conducting channel formed at the interface, which can limit the carrier mobility enhancement. In this work, we study the effect of the LaAlO₃ thickness on the transport properties in LaAlO₃/SrTiO₃ heterostructures by ionic liquid gating. We find that the transport properties of the LaAlO₃/SrTiO₃ interface are dominated by the intrinsic interactions rather than the LaAlO₃ thickness and possible effects from the ions in the liquid. We observe a Kondo effect, which is enhanced while increasing the gate voltage. We also observe a gate-tunable and temperature-dependent anomalous Hall effect, which always emerges near the Kondo temperature. Our experiments pave the way to manipulate the various magnetic interactions in LaAlO₃/SrTiO₃ heterostructures.

The two-dimensional electron system (2DES) at the interface between LaAlO₃ (LAO) and SrTiO₃ (STO) [1] has been the focus of intensive studies due to its intriguing properties, such as superconductivity [2], signatures of magnetism [3–5] and even their coexistence [6, 7]. It has also been demonstrated that the 2DES properties can be modulated by electrostatic gating. Pioneering works have been performed in the back-gate configuration, where the dielectric insulator is the STO substrate. Novel gate-tunable effects, such as insulator to metal transition [8], insulator to superconductor transition [9] and Rashba spin-orbit coupling [10, 11] have been reported. However, in this configuration high voltages of tens to hundreds of volts are required to achieve a sizeable gating effect. Moreover, the high voltages also induce unavoidable modifications to the defect landscape in the STO substrate [12]. The top-gate geometry works in a similar way as the back-gate counterpart, but the insulating dielectric is the LAO overlayer. Compared with back-gating, the big advantage of top-gating is that it requires very low voltages to achieve sizeable gating effects. However, the device fabrication process is very complicated which is due to the requirement of multiple aligned lithography steps [13].

Electric double layer transistors (EDLTs) of the top-gate configuration provide an alternative approach. In recent years, EDLTs have generated considerable research interest due to the capability of inducing high carrier densities in materials. EDLTs have been used for inducing superconductivity in STO [14] and KTaO₃ [15] as well as for tuning transport properties in LAO/STO heterostructures [16–18]. EDLTs use ionic liquids (ILs) as gate dielectrics, in which the size of the ions is usually larger than the lattice parameter of perovskite oxides. For instance, the average diameter of the ions in a widely used IL, called DEME-TFSI [19], is ~ 0.7 nm [20]. When the electrolyte touches the channel, the long-range Coulomb

potentials created by the ions will cause inevitable scattering of the conduction electrons and therefore limit the mobility enhancement, as was shown for experiments on BN-encapsulated graphene [21]. In a similar fashion, Gallagher *et al.* [22] have recently reported a ten-fold improvement of the carrier mobility in STO single crystals by covering the channel with a thin BN flake.

In LAO/STO heterostructures, the LAO film is a natural protection for the channel. However, one would expect that there is a trade-off between obtaining high carrier densities, which requires thin LAO layers, and achieving high mobilities, which requires thick LAO layers. In this work, we study the effect of LAO film thickness on the transport properties of three LAO/STO EDLTs. We obtain the largest tunability in a device with 4 unit cells (uc) of LAO. We observe a gate-tunable Kondo effect in all the devices. More interestingly, we also observe a temperature-dependent nonlinearity of the Hall resistance, which is always accompanied by the emergence of Kondo effect. We attribute this anomaly to an anomalous Hall effect. Our results imply that the transport properties of LAO/STO EDLTs are mainly governed by the intrinsic interactions, while the LAO thickness has a minor effect.

A schematic of the EDLT device is shown in Fig. 1(a). First, a sputtered amorphous AlO_x hard mask in form of a negative Hall bar geometry (thickness ~ 15 nm) was fabricated on a TiO₂-terminated STO (001) substrate by photolithography. Then, an LAO film was deposited at 800 °C in an Ar pressure of 0.04 mbar by 90° off-axis sputtering [23]. Finally, the sample was *in situ* annealed at 600 °C in 1 mbar of oxygen for 1 h. The length between two voltage probes is 500 μ m, and the Hall bar width is 50 μ m. It is well known that the critical thickness of LAO which gives rise to a conducting interface is 4 uc [8]. We fabricated three devices with different thickness of LAO layer. Since we do not have thickness monitoring

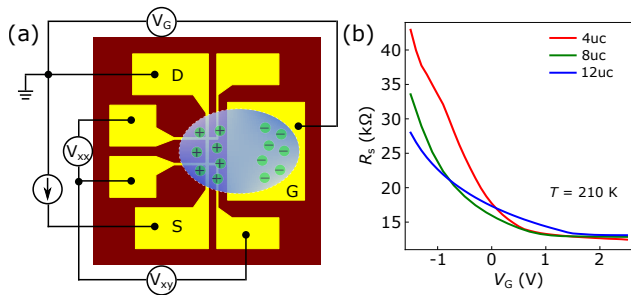


FIG. 1. (a) A schematic of the EDLT device. Source and drain are labeled as S and D. The longitudinal (V_{xx}) and transverse voltages (V_{xy}) are measured simultaneously. The gate voltage (V_G) is applied between the gate electrode (G) and the drain. (b) Sheet resistance (R_s) as a function of V_G at 210 K for the three devices with different thickness of the LAO layer as indicated.

capability during growth, we used the calibrated growth rate of $4.3 \text{ \AA}/\text{min}$ [23] to estimate the thickness. Growth times were 3.5, 7.0 and 10.5 min, respectively, yielding the devices with thicknesses of 1.5, 3.0 and 4.5 nm, which we refer to as 4uc, 8uc and 12uc [24]. After sample fabrication, a droplet of IL, DEME-TFSI (IOLITEC), was applied onto the device surface covering the gate electrode and the channel.

The magnetotransport measurements were performed in a Physical Property Measurement System (Quantum Design) at temperatures down to 3 K and magnetic fields up to 9 T. As shown in Fig. 1(a), a Keithley 6221 current source was used to apply a direct current ($I_{DC} = 1.0 \mu\text{A}$). Two Keithley 2182A nanovoltmeters were used to measure the longitudinal (V_{xx}) and transverse voltages (V_{xy}). The gate voltage (V_G) was applied by a Keithley 2400 source meter. The freezing point of DEME-TFSI is $\sim 180 \text{ K}$. As a general procedure, we applied V_G at 210 K and then waited for $\sim 15 \text{ min}$ for the IL to equilibrate. The measurements were started at 150 K and the leakage current was less than 1.0 nA during the measurements.

Fig. 1(b) shows the sheet resistance (R_s) as a function of V_G at 210 K for the three devices. As expected, the gate tuning effect on R_s decreases as the LAO thickness increases. Above $V_G = 1.5 \text{ V}$, R_s almost saturates in all of the devices. We find that the gate voltage sweeps are nicely reproducible, which allows us to exclude any possible electrochemical reaction occurring on LAO surface [14]. The forward and backward sweeps are also reversible, indicating that no electron trapping [12] is induced in the top-gate configuration.

First, we present the temperature dependence of R_s measured under various values of V_G . Fig. 2(a) shows the data of device 4uc [24]. At $V_G = 0 \text{ V}$, R_s first decreases from 150 K to 10 K and then remains unchanged. In the negative voltage regime, R_s decreases monotonously to 3 K, but in the positive voltage regime, R_s first reaches a minimum at $\sim 30 \text{ K}$ and then increases as temperature decreases to 3 K. For a better view, the resistance relative

to its value at 3 K, $R_s(T) - R_s(3 \text{ K})$, is plotted in the inset of Fig. 2(a). In earlier reports, this resistance upturn has been attributed to either a weak localization (WL) effect [9, 25] or a Kondo effect [16, 26]. Fig. 2(b) shows the magnetoresistance (MR) of device 4uc measured at 3 K and under various V_G s [24]. The MR curves exhibit sharp cusps in low magnetic fields, which is the characteristic feature of a weak antilocalization (WAL) effect [27] and allows us to exclude the WL effect.

In a metallic system where itinerant electrons couple antiferromagnetically with localized moments, spin-flip scattering gives rise to a resistance minimum, which is known as the Kondo effect [28]. The Kondo effect is characterized by a Kondo temperature, T_K . For $T < T_K$, the resistance increases logarithmically and eventually saturates at low temperatures. The $R_s(T)$ can be described by a simple formula [26]

$$R(T) = R_0 + aT^2 + bT^5 + R_K(T/T_K), \quad (1)$$

where R_0 is the residual resistance, and the T^2 and T^5 terms represent the temperature-dependent electron-electron and electron-phonon interactions, respectively. $R_K(T/T_K)$ is the universal resistivity function with the empirical form

$$R_K(T/T_K) = R_K(0 \text{ K}) \left(\frac{1}{1 + (2^{1/s} - 1)(T/T_K)^2} \right)^s, \quad (2)$$

where $R_K(0 \text{ K})$ is the Kondo resistance at zero temperature and $s = 0.225$. Fig. 2(c) shows the fitting results of device 4uc at $V_G = 1 \text{ V}$ and 2 V . The extracted values of R_0 , $R_K(0 \text{ K})$ and T_K as a function of V_G for the three devices are plotted in Fig. 2(d)-(f).

Numerical renormalization group (NRG) method normalizes the Kondo contribution to the transport by a universal parameter T/T_K [29]. It is often used as a criterion to verify the Kondo scenario. As shown in the inset of Fig. 2(c), $R_K(T/T_K)/R_K(0 \text{ K})$ as a function of T/T_K measured under various V_G s of the three devices all collapse into a single curve, which confirms that the Kondo effect is the origin of the observed resistance minimum [24]. As can be seen from Fig. 2(e)-(f) in particular, $R_K(0 \text{ K})$ and T_K are a function of the gate voltage. Such a gate-tunable Kondo effect has been previously observed in undoped STO single crystals [26], LAO/STO [16] and $\gamma\text{-Al}_2\text{O}_3/\text{STO}$ [30] EDLTs, and is consistent with our results. It is noteworthy to mention that the Kondo effect is caused by the interaction between itinerant electrons and localized electrons [26] rather than with conventional magnetic impurities, such as iron. In the presence of magnetic impurities, one would expect to observe a stronger Kondo effect at a lower carrier density, not the opposite trend seen here.

Next, we present the temperature-dependent nonlinearity of the Hall resistance (R_{xy}) measured under various V_G s. Fig. 3(a) shows R_{xy} as a function of magnetic field (B) of device 4uc measured at various temperatures and at $V_G = 2 \text{ V}$ [24]. The $R_{xy}(B)$ curves are separated

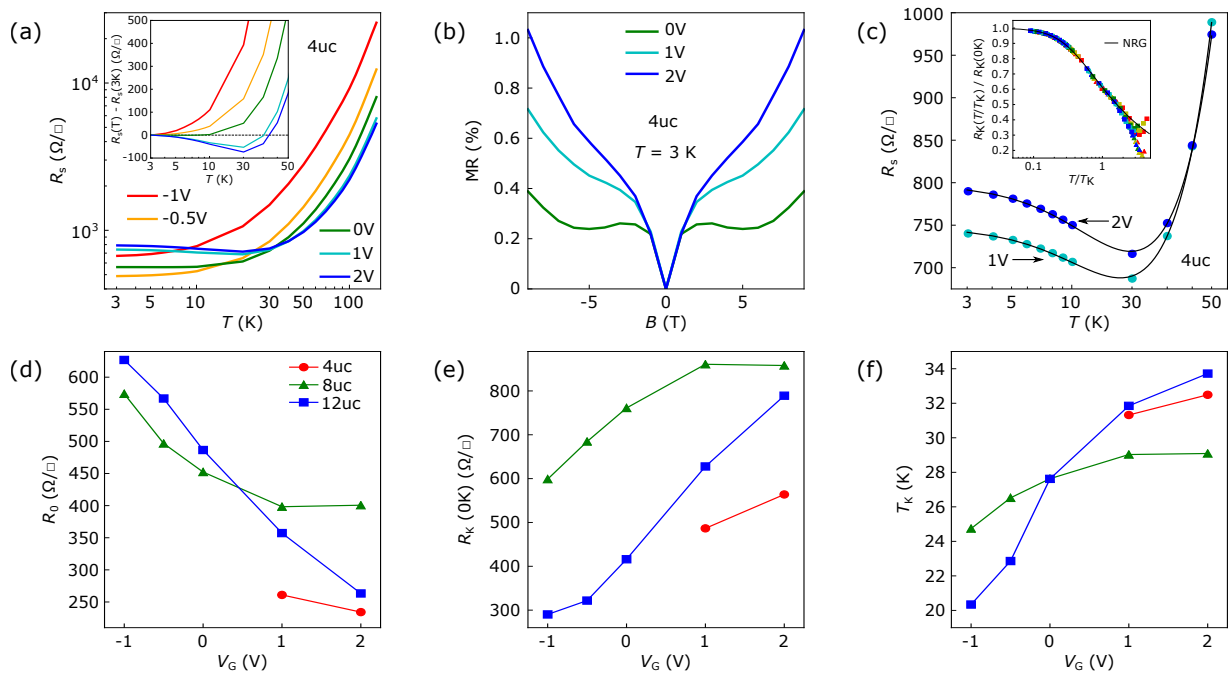


FIG. 2. (a) R_s as a function of temperature at various V_G s of device 4uc. The inset shows the resistance relative to its value at 3 K, $R_s(T) - R_s(3\text{K})$. (b) Magnetoresistance (MR) at various V_G s of device 4uc at 3 K. (c) R_s minimum observed from 3 to 50 K of device 4uc at 1 V and 2 V. The black lines are the Kondo effect fits using Eqs. (1) and (2). The inset shows the normalized Kondo resistance ($R_K(T/T_K)/R_K(0\text{K})$) versus the reduced temperature (T/T_K) curves of the three devices collapse into a single black line, which is obtained from the numerical renormalization group (NRG) method. (d)-(f) Extracted Kondo parameters, (d) the residual resistance (R_0), (e) the Kondo resistance at zero temperature ($R_K(0\text{K})$) and (f) the Kondo temperature (T_K), as a function of V_G of the three devices.

by an offset of 50Ω for clarity and the black lines are their linear fits. It can be seen that the $R_{xy}(B)$ curves are linear at high temperatures (above 50 K) and low temperatures (below 10 K), but nonlinear at intermediate temperatures. We find that the emergence of nonlinear $R_{xy}(B)$ is always accompanied by the observation of Kondo effect. For the cases of device 4uc at $V_G = -1\text{V}$, -0.5V and 0V , $R_{xy}(B)$ curves are linear at all temperatures.

One possibility for a nonlinear Hall effect is two-band transport [13, 31]. The band structure of the LAO/STO interface is formed by the Ti t_{2g} orbitals. For LAO films grown on STO (001) substrates, the d_{xy} band stays below the $d_{xz,yz}$ bands in energy [13, 32, 33]. In the one-band regime, only the d_{xy} band is populated. The carrier density (n_s) and mobility (μ) can be determined by $n_s = B/eR_{xy}$ and $\mu = R_{xy}/BR_s$, where e is the electron charge. Tuning the Fermi level to above the bottom of the $d_{xz,yz}$ bands triggers a Lifshitz transition, resulting in a nonlinear $R_{xy}(B)$. In the two-band regime, the carrier densities and mobilities can be extracted by fitting the magnetotransport data with a two-band model [13]

$$\sigma_{xx} = e \sum_{i=1,2} \frac{n_i \mu_i}{1 + (\mu_i B)^2}; \quad \sigma_{xy} = eB \sum_{i=1,2} \frac{n_i \mu_i^2}{1 + (\mu_i B)^2}, \quad (3)$$

where n_i and μ_i are the carrier density and mobility of

the i th band.

Fig. 3(b) plots the carrier density as a function of temperature of device 4uc at $V_G = 2\text{V}$ as an example. It can be seen that the total carrier density ($n_s = n_1 + n_2$) is $2.86 \times 10^{13} \text{cm}^{-2}$ at 3 K and increases to $4.03 \times 10^{13} \text{cm}^{-2}$ at 30 K, corresponding to an increase of $\sim 41\%$. In earlier reports, such a nonlinear Hall effect at intermediate temperatures has been only reported in a 26 uc LAO/STO sample [34], where the occupation of the $d_{xz,yz}$ bands has been attributed to thermally excited electrons. However, we argue that this cannot serve as a convincing explanation for our results. First, when the 2DES enters the nonlinear regime, we obtain a large increase of n_s , ranging from 22% to 41%, in our three devices at various V_G s. But in Ref. [34], the increase is only $\sim 3\%$, which is much less than our case. Second, for the cases of device 4uc at $V_G = -1\text{V}$, -0.5V and 0V , we find that n_s remains almost constant at all temperatures. If thermal excitation indeed gives rise to additional electrons, one would expect to observe an increase of n_s under all V_G s. Third, in earlier reports, the critical carrier density (n_L) window for Lifshitz transition is $1.5\text{--}2.9 \times 10^{13} \text{cm}^{-2}$ [12, 13, 31]. Within our measurement limit, we observe linear $R_{xy}(B)$ at 3 K in all of the devices. Fig. 3(c) shows the extracted $n_s(3\text{K})$ as a function of V_G . The threshold carrier density for the emergence of Kondo effect differs among devices, but

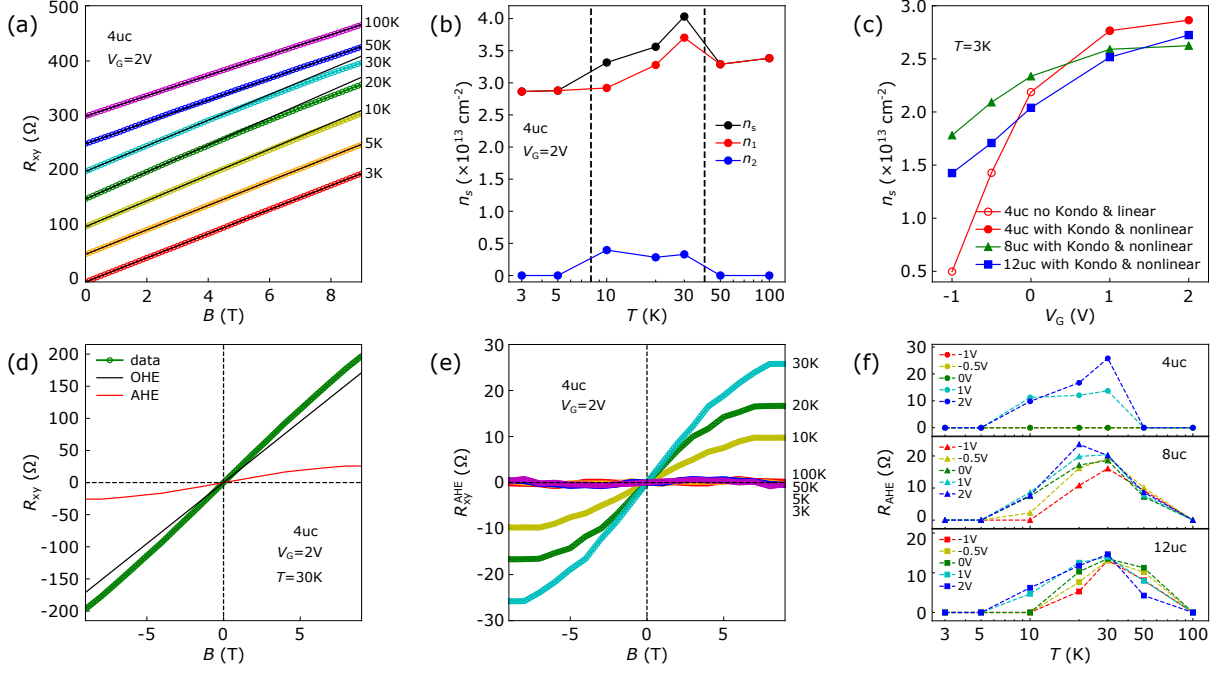


FIG. 3. (a) Hall resistance (R_{xy}) at various temperatures of device 4uc at $V_G = 2$ V. The curves are separated by an offset of 50Ω and the black lines are linear fits to R_{xy} . (b) Temperature dependence of the carrier density (n_s) of device 4uc at $V_G = 2$ V. The values are extracted by fitting the magnetotransport data with a two-band model. n_1 and n_2 represent the carrier densities of different conduction channels and their sum is n_s . (c) n_s as a function of V_G of the three devices at 3 K. (d) An example for the determination of OHE and AHE terms from R_{xy} measured on device 4uc at 30 K and $V_G = 2$ V. (e) Deduced AHE as a function of magnetic field at various temperatures of device 4uc at $V_G = 2$ V. (f) Anomalous Hall resistance (R_{AHE}) as a function of temperature at various V_G s of the three devices.

the overall trend is the same. Most of the values are in the n_L window, which indicates that a higher magnetic field is required to reliably analyze the transport regime. However, even the 2DES is in the two-band regime, we should expect to see the nonlinearity appearing in magnetic fields higher than 9 T, rather than the extraordinary behavior observed here.

An alternative possibility for the nonlinear Hall effect is the anomalous Hall effect (AHE), which occurs in solids with ferromagnetic order [35]. In a system with AHE, R_{xy} is consisted of the ordinary Hall effect (OHE) term and the AHE term. As shown in Fig. 3(d), the OHE term, R_{xy}^{OHE} , can be obtained from a linear fit to the high field limit of R_{xy} . Subtracting R_{xy}^{OHE} from R_{xy} will give the AHE term, R_{xy}^{AHE} [36]. Fig. 3(e) shows the R_{xy}^{AHE} terms obtained at various temperatures for device 4uc at $V_G = 2$ V. Similar to common observations in the LAO/STO system, the R_{xy}^{AHE} curves show no hysteresis. Gunkel *et al.* [37] have proposed a phenomenological Langevin-type function to describe the R_{xy}^{AHE} . However, we could not obtain a satisfactory fit due to the lack of a clear magnetization saturation in the limited magnetic field. Christensen *et al.* [38] have recently reported a non-saturating AHE even up to 15 T. Fig. 3(f) shows the anomalous Hall resistance (R_{AHE}) taken from the high field limit of R_{xy}^{AHE} , which increases as V_G is increasing.

Similar temperature-dependent AHE effect has been reported in STO single crystals [39] and LAO/STO:Fe heterostructures [40]. Fig. 4(a) and 4(b) plot the n_s and μ as a function of temperature of device 4uc under various V_G s. Device 8uc and 12uc show similar behavior with less tunability [24].

The Kondo effect originates from antiferromagnetic coupling between itinerant electrons and localized spins [28]. In our LAO/STO system, the Kondo scattering centers are localized and unpaired electrons [26]. The density of these localized electrons increases when increasing V_G . The temperature range in which AHE emerges is closely related to T_K . At low temperatures, $T \ll T_K$, the localized spins are effectively screened by the continuum states of the metal host upon forming coherent many-body singlet states [41]. A rough estimation of the energy scale, $g\mu_B B \approx k_B T_K$ (g is the g factor, μ_B is the Bohr magneton and k_B is the Boltzmann constant), indicates that a magnetic field of several tens of Tesla is required to break down the Kondo screening. Therefore a linear R_{xy} is observed. At high temperatures, $T \gg T_K$, the alignment of localized moments by magnetic field is countered by thermal fluctuations, resulting in a linear R_{xy} as well. At intermediate temperatures, $T \sim T_K$, the polarization of localized spins by magnetic field could give rise to a ferromagnetic ordering, resulting in the anomalous Hall effect. The origin of this non-hysteretic magnetization is

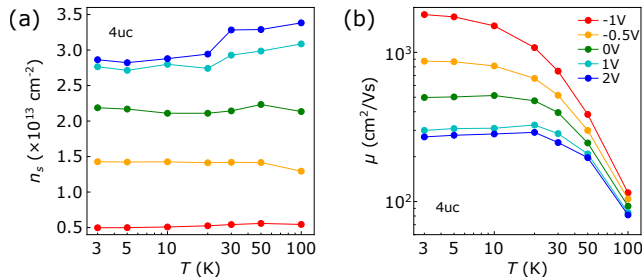


FIG. 4. (a) Temperature dependence of (a) carrier density (n_s) and (b) mobility (μ) of device 4uc at various V_{GS} . The values are obtained by fitting R_{xy}^{OHE} .

still unclear. It may be due to spiral magnetic ordering [42] or polarization of unpaired spins [43, 44].

In conclusion, we have studied the effect of LAO film thickness on the transport properties of LAO/STO EDLTs, and obtained the largest tunability in terms of carrier density and mobility in the device with 4 uc of

LAO. We have shown a gate-tunable Kondo effect which originates from localized electrons. More interestingly, we have also observed a gate-tunable anomalous Hall effect which always emerges near the Kondo temperature. Our results show that the physical properties of LAO/STO EDLTs are dominated by the intrinsic interactions, while the LAO thickness has a secondary effect. Our experiments provide insights to understand the observed magnetism at the LAO/STO interface and demonstrate a non-trivial tuning of magnetic interactions by ionic liquid gating, paving the way for designing novel electronic devices based on LAO/STO heterostructures.

We thank Jan van Ruitenbeek, Yun-Yi Pai, Shengwei Zeng, Yu Zhang, Nikita Lebedev and Aymen Ben Hamida for useful discussions. We also thank Johannes Jobst, Hasan Atesci and Jan van Ruitenbeek for their technical support. This work is supported by the Netherlands Organisation for Scientific Research (NWO). C. Y. is supported by China Scholarship Council (CSC) with grant No. 201508110214.

-
- [1] A. Ohtomo and H. Y. Hwang, *Nature* **427**, 423 (2004).
- [2] N. Reyren, S. Thiel, A. D. Caviglia, L. F. Kourkoutis, G. Hammerl, C. Richter, C. W. Schneider, T. Kopp, A.-S. Ruetschi, D. Jaccard, M. Gabay, D. A. Muller, J.-M. Triscone, and J. Mannhart, *Science* **317**, 1196 (2007).
- [3] A. Brinkman, M. Huijben, M. V. Zalk, J. Huijben, U. Zeitler, J. C. Maan, W. G. V. D. Wiel, G. Rijnders, D. H. A. Blank, and H. Hilgenkamp, *Nature Materials* **6**, 493 (2007).
- [4] Ariando, X. Wang, G. Baskaran, Z. Q. Liu, J. Huijben, J. B. Yi, A. Annadi, A. R. Barman, A. Rusydi, S. Dhar, Y. P. Feng, J. Ding, H. Hilgenkamp, and T. Venkatesan, *Nature Communications* **2**, 188 (2011).
- [5] J.-S. Lee, Y. W. Xie, H. K. Sato, C. Bell, Y. Hikita, H. Y. Hwang, and C.-C. Kao, *Nature Materials* **12**, 703 (2013).
- [6] L. Li, C. Richter, J. Mannhart, and R. C. Ashoori, *Nature Physics* **7**, 762 (2011).
- [7] J. A. Bert, B. Kalisky, C. Bell, M. Kim, Y. Hikita, H. Y. Hwang, and K. A. Moler, *Nature Physics* **7**, 767 (2011).
- [8] S. Thiel, G. Hammerl, A. Schmehl, C. W. Schneider, and J. Mannhart, *Science* **313**, 1942 (2006).
- [9] A. D. Caviglia, S. Gariglio, N. Reyren, D. Jaccard, T. Schneider, M. Gabay, S. Thiel, G. Hammerl, J. Mannhart, and J.-M. Triscone, *Nature* **456**, 624 (2008).
- [10] M. B. Shalom, M. Sachs, D. Rakhmilevitch, A. Palevski, and Y. Dagan, *Physical Review Letters* **104**, 126802 (2010).
- [11] A. D. Caviglia, M. Gabay, S. Gariglio, N. Reyren, C. Cancellieri, and J.-M. Triscone, *Physical Review Letters* **104**, 126803 (2010).
- [12] C. Yin, A. E. M. Smink, I. Leermakers, L. M. K. Tang, N. Lebedev, U. Zeitler, W. G. van der Wiel, H. Hilgenkamp, and J. Aarts, (2019), [arXiv:1902.007648](https://arxiv.org/abs/1902.007648).
- [13] A. E. M. Smink, J. C. de Boer, M. P. Stehno, A. Brinkman, W. G. van der Wiel, and H. Hilgenkamp, *Physical Review Letters* **118**, 106401 (2017).
- [14] K. Ueno, S. Nakamura, H. Shimotani, A. Ohtomo, N. Kimura, T. Nojima, H. Aoki, Y. Iwasa, and M. Kawasaki, *Nature Materials* **7**, 855 (2008).
- [15] K. Ueno, S. Nakamura, H. Shimotani, H. T. Yuan, N. Kimura, T. Nojima, H. Aoki, Y. Iwasa, and M. Kawasaki, *Nature Nanotechnology* **6**, 408 (2011).
- [16] W.-N. Lin, J.-F. Ding, S.-X. Wu, Y.-F. Li, J. Lourembam, S. Shannigrahi, S.-J. Wang, and T. Wu, *Advanced Materials Interfaces* **1**, 1300001 (2014).
- [17] S. Zeng, W. Lü, Z. Huang, Z. Liu, K. Han, K. Gopinadhan, C. Li, R. Guo, W. Zhou, H. H. Ma, L. Jian, T. Venkatesan, and Ariando, *ACS Nano* **10**, 4532 (2016).
- [18] Z. Chen, H. Yuan, Y. Xie, D. Lu, H. Inoue, Y. Hikita, C. Bell, and H. Y. Hwang, *Nano Letters* **16**, 6130 (2016).
- [19] The molecular formula of DEME-TFSI is N, N-diethyl-N-methyl-N-(2-methoxyethyl)-ammonium bis(trifluoromethylsulfonyl)-imide.
- [20] Y.-J. Kim, Y. Matsuzawa, S. Ozaki, K. C. Park, C. Kim, M. Endo, H. Yoshida, G. Masuda, T. Sato, and M. S. Dresselhaus, *Journal of The Electrochemical Society* **152**, A710 (2005).
- [21] T. A. Petach, K. V. Reich, X. Zhang, K. Watanabe, T. Taniguchi, B. I. Shklovskii, and D. Goldhaber-Gordon, *ACS Nano* **11**, 8395 (2017).
- [22] P. Gallagher, M. Lee, T. A. Petach, S. W. Stanwyck, J. R. Williams, K. Watanabe, T. Taniguchi, and D. Goldhaber-Gordon, *Nature communications* **6**, 6437 (2015).
- [23] C. Yin, D. Krishnan, N. Gauquelin, J. Verbeeck, and J. Aarts, *Physical Review Materials* **3**, 034002 (2019).
- [24] See Supplemental Material for AFM images, sheet resistance as a function of temperature, NRG analysis, magnetoresistance, Hall resistance, carrier density and mobility of the three devices.

- [25] F. J. Wong, R. V. Chopdekar, and Y. Suzuki, *Physical Review B* **82**, 165413 (2010).
- [26] M. Lee, J. R. Williams, S. Zhang, C. D. Frisbie, and D. Goldhaber-Gordon, *Physical review letters* **107**, 256601 (2011).
- [27] P. Seiler, J. Zabaleta, R. Wanke, J. Mannhart, T. Kopp, and D. Braak, *Physical Review B* **97**, 075136 (2018).
- [28] J. Kondo, *Progress of Theoretical Physics* **32**, 37 (1964).
- [29] R. Bulla, T. A. Costi, and T. Pruschke, *Reviews of Modern Physics* **80**, 395 (2008).
- [30] W. Niu, Y. Zhang, Y. Gan, D. V. Christensen, M. V. Soosten, E. J. Garcia-Suarez, A. Riisager, X. Wang, Y. Xu, R. Zhang, N. Pryds, and Y. Chen, *Nano letters* **17**, 6878 (2017).
- [31] A. Joshua, S. Pecker, J. Ruhman, E. Altman, and S. Ilani, *Nature Communications* **3**, 1129 (2012).
- [32] M. Salluzzo, J. C. Cezar, N. B. Brookes, V. Bisogni, G. M. D. Luca, C. Richter, S. Thiel, J. Mannhart, M. Huijben, A. Brinkman, G. Rijnders, and G. Ghiringhelli, *Physical Review Letters* **102**, 166804 (2009).
- [33] A. F. Santander-Syro, O. Copie, T. Kondo, F. Fortuna, S. Pailhès, R. Weht, X. G. Qiu, F. Bertran, A. Nicolaou, A. Taleb-Ibrahimi, P. Le Fèvre, G. Herranz, M. Bibes, N. Reyren, Y. Apertet, P. Lecoeus, A. Barthélémy, and M. J. Rozenberg, *Nature* **469**, 189 (2011).
- [34] V. K. Guduru, A. McCollam, A. Jost, S. Wenderich, H. Hilgenkamp, J. C. Maan, A. Brinkman, and U. Zeitler, *Physical Review B* **88**, 241301 (2013).
- [35] N. Nagaosa, J. Sinova, S. Onoda, A. H. Macdonald, and N. P. Ong, *Reviews of Modern Physics* **82**, 1539 (2010).
- [36] D. Stornaiuolo, C. Cantoni, G. M. De Luca, R. Di Capua, E. D. Gennaro, G. Ghiringhelli, B. Jouault, D. Marrè, D. Massarotti, F. M. Granozio, I. Pallecchi, C. Piamonteze, S. Rusponi, F. Tafuri, and M. Salluzzo, *Nature materials* **15**, 278 (2016).
- [37] F. Gunkel, C. Bell, H. Inoue, B. Kim, A. G. Swartz, T. A. Merz, Y. Hikita, S. Harashima, H. K. Sato, M. Minohara, S. Hoffmann-Eifert, R. Dittmann, and H. Y. Hwang, *Physical Review X* **6**, 031035 (2016).
- [38] D. V. Christensen, Y. Frenkel, Y. Z. Chen, Y. W. Xie, Z. Y. Chen, Y. Hikita, A. Smith, L. Klein, H. Y. Hwang, N. Pryds, and B. Kalisky, *Nature Physics* (2018), 10.1038/s41567-018-0363-x.
- [39] Y. Lee, C. Clement, J. Hellerstedt, J. Kinney, L. Kinischtzke, X. Leng, S. D. Snyder, and A. M. Goldman, *Physical Review Letters* **106**, 136809 (2011).
- [40] H. Zhang, X. Yan, H. Zhang, F. Wang, Y. Gu, X. Ning, T. Khan, R. Li, Y. Chen, W. Liu, S. Wang, B. Shen, and J. Sun, *Physical Review B* **97**, 155150 (2018).
- [41] P. Nozières, *Journal of Low Temperature Physics* **17**, 31 (1974).
- [42] S. Banerjee, O. Erten, and M. Randeria, *Nature Physics* **9**, 626 (2013).
- [43] G. Cheng, M. Tomczyk, S. Lu, J. P. Veazey, M. Huang, P. Irvin, S. Ryu, H. Lee, C.-B. Eom, C. S. Hellberg, and J. Levy, *Nature* **521**, 196 (2015).
- [44] Y.-Y. Pai, A. Tylan-Tyler, P. Irvin, and J. Levy, (2016), [arXiv:1610.00789](https://arxiv.org/abs/1610.00789).